RESEARCH ARTICLE

Editorial Process: Submission:01/16/2025 Acceptance:10/04/2025 Published:10/16/2025

Protective Effects of Aqueous Extract of *Myrtus communis L*. Leaves against Oxidative Susceptibility of Rat Plasma and Hemoglobin during Exposure to X-ray Radiation

Hadi Ansari, Fatemeh Seif, Mohamad Reza Bayatiani*

Abstract

Background: Ionizing radiation such as X-rays generates reactive oxygen species (ROS), leading to oxidative stress and damage to biomolecules including hemoglobin and plasma proteins. This study aimed to evaluate the protective effects of the aqueous extract of Myrtus communis L. leaves against oxidative alterations caused by X-ray exposure. Materials and Methods: Twenty-four adult male Wistar rats were randomly assigned to control, X-ray exposed, and extract-treated plus X-ray exposed groups. The Myrtus communis extract (0.5 mg/kg) was administered intraperitoneally for 7 consecutive days. Rats in the experimental group were exposed to 6 MV X-ray radiation, and blood samples were collected one hour post-exposure. Oxidative modifications of hemoglobin (Hb) were analyzed, and plasma oxidative stress markers including protein carbonyl (PCO), malondialdehyde (MDA), and ferric reducing antioxidant power (FRAP) were measured. Artificial neural network (ANN) models were developed to identify key predictors of oxyhemoglobin (OxyHb) concentration. Results: X-ray exposure significantly increased levels of methemoglobin (metHb) and hemichrome (HMC), while reducing absorbance at 340 nm (globin-heme interaction), 420 nm (Soret band), 542 nm (OxyHb), and 577 nm (heme-heme interaction). Plasma MDA and PCO levels were also significantly elevated. MDA showed a negative correlation with OxyHb and a positive correlation with both metHb and HMC concentrations. Administration of Myrtus communis extract effectively mitigated these oxidative changes. ANN analysis revealed that absorbance at 577 and 560 nm, metHb levels, the A577/A542 ratio, and HMC were the strongest predictors of OxyHb concentration. Conclusions: The aqueous extract of Myrtus communis L. leaves offers significant protection against X-ray-induced oxidative damage to hemoglobin and plasma. Moreover, ANN models can effectively identify biomarkers associated with oxidative stress in irradiated blood, with potential clinical implications for radiotherapy patients.

Keywords: Hemoglobin- Myrtus communis- Oxidative stress- Plasma- X-ray radiation

Asian Pac J Cancer Prev, 26 (10), 3641-3652

Introduction

The ionizing radiation can damage the living organisms in two main ways: 1) damage to the cellular DNA, shown as single-strand breaks, double-strand breaks and impaired bases [1]. 2) production of free radicals from water due to radiolysis can damage biological molecules and imbalance Oxidation [2, 3]. In addition, ionizing radiation can change biological mechanisms such as: altering immune function [4] starting cell signaling [5] and increasing bystander effect [6]; which is of less importance to oxidative stress.

Reduction of unintended exposure is correlated with decreased accumulation of reactive oxygen species (ROS) which can improve DNA protection [7]. The excessive exposure might happen because of a radiation accident or leakage in radiotherapy, radiology, nuclear medicine and nuclear power plants. Also, primary or scattered

radiation in radiotherapy and x-ray imaging can cause secondary cancer in healthy organs [8]. Three principles for radiation protection comprises time, distance, and shielding. But these roles lose their efficiency in unpredictable and unwanted exposures. Therefore, using chemical and pharmaceutical radioprotectors is necessary to prevent the harmful effect of ionizing radiation on the general public health and normal tissues of the patient. The precautionary and therapeutic proceeding may be achieved using pharmaceutical radioprotectors before and after the exposure [9]. The major problem of the chemical radioprotectors is their clinical concentration toxicity and their time limitation to be used after the exposure [10, 11]. Therefore, in non-clinical situations, which are mostly accidental and unplanned, they cannot be invested appropriately [12].

Utilization of herbal products and their derivatives as

Radiotherapy and Medical Physics Department, Arak University of Medical Sciences, Arak, Iran. *For Correspondence: bayatiani@arakmu.ac.ir. Hadi Ansarihadipour and Fatemeh Seifhave have equal contribution in this study.

radioprotectors associated with synthetic chemicals has some advantages including being cheap and accessible, uncomplicated techniques in generating process, known and defined side effects and being non-toxic in optimal concentrations [13, 14].

Many researches have been done to address the radioprotective potential of herbal plants and their derivatives. It has been shown that utilizing 20 mg/kg of abana 1 hour before exposure of 7 Gy and 12 Gy of gamma rays can reduce the mortality and indication of hematological and GI syndromes in irradiated mice and increase dose modification factor to 1.2 and event threshold to 1.8 Gy [15]. Doses of 250 and 500mg/kg of Polyalthia longifolia leaves extract for 15 days before radiation (10 Gy, 6MV X-rays) can improve hematological parameters and increase spleen colony forming units in mice. It also can decrease the high rate of ALT, AST, and bilirubin in livers of exposed mice [16]. Previous studies have shown antioxidant activity of the extracts from Myrtus leaf, stem and flower [17, 18]. Wannes WA et al reported the highest total phenol contents and flavonoids were observed in essential oils from Myrtus leaf and stem respectively [19]. Also, The anti-mutagenic activity of Myrtus extract has been investigated and the results showed that ethyl acetate and methanol extracts have the maximum protection against mutagens sodium azide and aflatoxin B1 (AFB1) in Salmonella typhimurium strains TA100 and TA98 [20]. Jabri et al has shown the therapeutic properties of the Myrtus plant. The results of this study indicated that the aqueous extract of Myrtus seeds can provide protection against oxidation and microbial diarrhea induced by castor oil in infected rat. In this research, the antioxidant properties of the Myrtus were assessed by measuring the activity of SOD, CAT (B) and GPx enzymes by HPLC-PDA-ESI-MS / MS and lipid anti-oxidation properties were estimated by MDA assay and the role of phenolic compounds was emphasized [21]. Phenolic derivatives are divided into three main categories: hydroxybenzoic acid, anthocyanins and flavanols. The results of Ines et al showed that the purified 3,5-O-di-galloylquinic acid, abstracted from Myrtus leaves, can reduce lipid peroxidation induced by H₂O₂ up to 82.2% in the K562 cell line. Also, the results of the comet assay showed that using a purified molecule with a concentration of 400 µg ml-1, the tail extent moment can be decreased up to 50% in the group receiving the derived molecule compared to the H2O2 receptor group [22].

Tumen et al studied the effects of Myrtus extract in dichloromethane (DCM), acetone, ethyl acetate and methanol on the activity of acetylcholinesterase, butyrylcholinesterase and tyrosinase enzymes. Results showed that Polar extracts can be effective in reacting with 2,2-diphenyl-1-picyrylhydrazyl (DPPH) and N, N-dimethyl-p-phenylenediamine (DMPD) radicals and the dichloromethane extract of the berries can provide an appropriate metal chelation capacity. The study concluded that the derivatives of the Myrtus herb can be used as a neuroprotective agent [23].

In the present study, aqueous extract of Myrtus communis L. leaves were administered to rats prior to X-ray exposure to evaluate its potential activity as a

radioprotective agent, with its protective effects assessed through various oxidative and antioxidative parameters. The derivatives of hemoglobin (Hb) were analyzed by measuring the concentrations of oxyHb, metHb, and HMC, while Hb spectrum were analyzed in the range of 300 to 700 nm. Oxidative status in plasma were evaluated by measuring protein carbonyls (PCO), malondialdehyde (MDA), and antioxidant capacity using the ferric reducing ability of plasma (FRAP). Additionally, artificial neural network (ANN) models were developed to identify predictive parameters for estimating the concentration of OxyHb derivatives and plasma oxidant and antioxidant parameters.

Materials and Methods

Figure 1 illustrates the study design summary including treatment groups, oxidative and antioxidative parameters and Figure 2 shows the artificial neural network.

Laboratory Animals

Twenty-four adults male Wistar rats, aged 3 months and weighing 210 ± 10 g, were maintained under controlled conditions for temperature, humidity, lighting, and food and water ad libitum. The rats were randomly divided in three groups: 1) the control group, which remained under normal conditions without any exposure to X-rays; 2) the X-ray group, which received an 6 Gy of X-rays produced by a linear accelerator; and 3) the X-ray and Myrtus group, which was exposed to X-rays following the daily intraperitoneal administration of 0.5 mg/kg of aqueous extract of Myrtus communis L. leave. Finally, Blood samples were collected from heart and the concentration of Hb derivatives, FRAP, MDA and carbonyl content of plasma proteins were determined according to biochemical analyses.

X-ray Irradiation

The whole-body radiation (WBR) was delivered to the rats as a single fraction of 6Gy of X-rays. The radiation was produced by a 6-MV linear accelerator (Elekta compact, Arak Khansari Hospital). The dose rate was 350 cGy/MU. The radiation field size was 30cm ×30cm at a source distance of 100 cm.

Structural changes in Hemoglobin

Conformational modifications of hemoglobin (Hb) were analyzed spectrophotometrically at the range of 300 to 700 nm. The following equations were used to calculate the concentrations of oxyhemoglobin (oxyHb), methemoglobin (metHb), and HMC [25]:

OxyHb=119A577-39A630 -89A560

MetHb= 28A577+307A630 -55A560

HMC= -133577-114A630 +233A560

Abbreviation A stands for optical absorption at the indicated wavelengths.

The absorbance spectra of hemoglobin reveal several distinctive bands: 1) choleglobin is indicated by a rise in absorbance at 700 nm, 2) met-Hb shows a shoulder at 630 nm, 3) ferryl Hb can be identified by the absence of this shoulder, 4) oxyHb is present at the 577 and 542 nm bands,

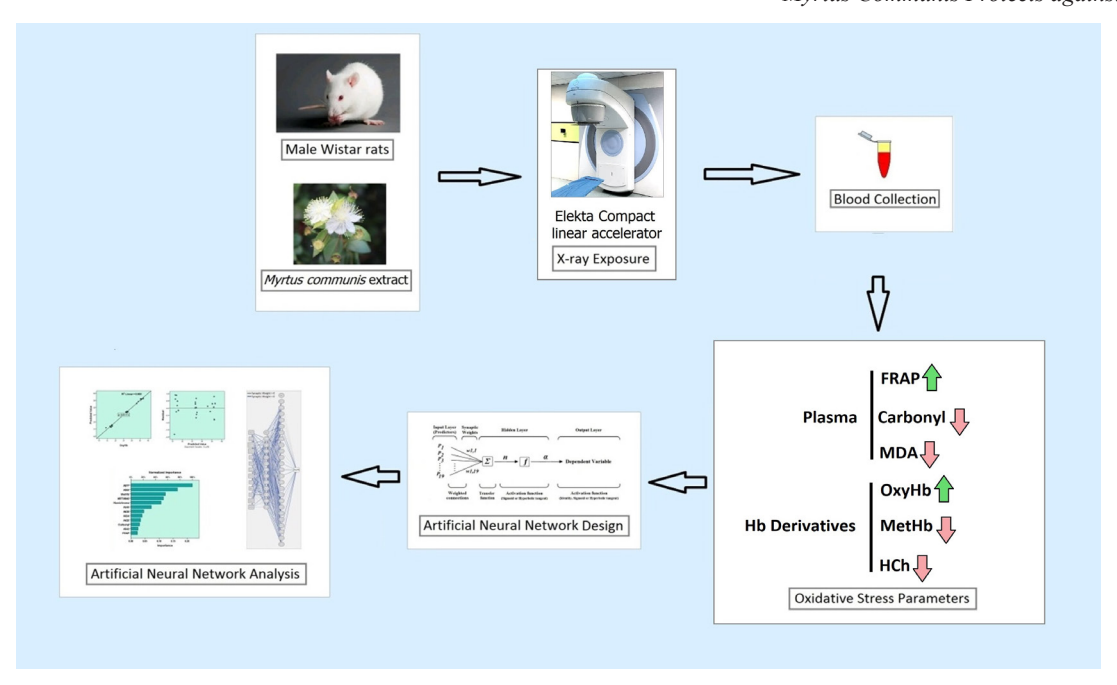


Figure 1. Graphical Abstract

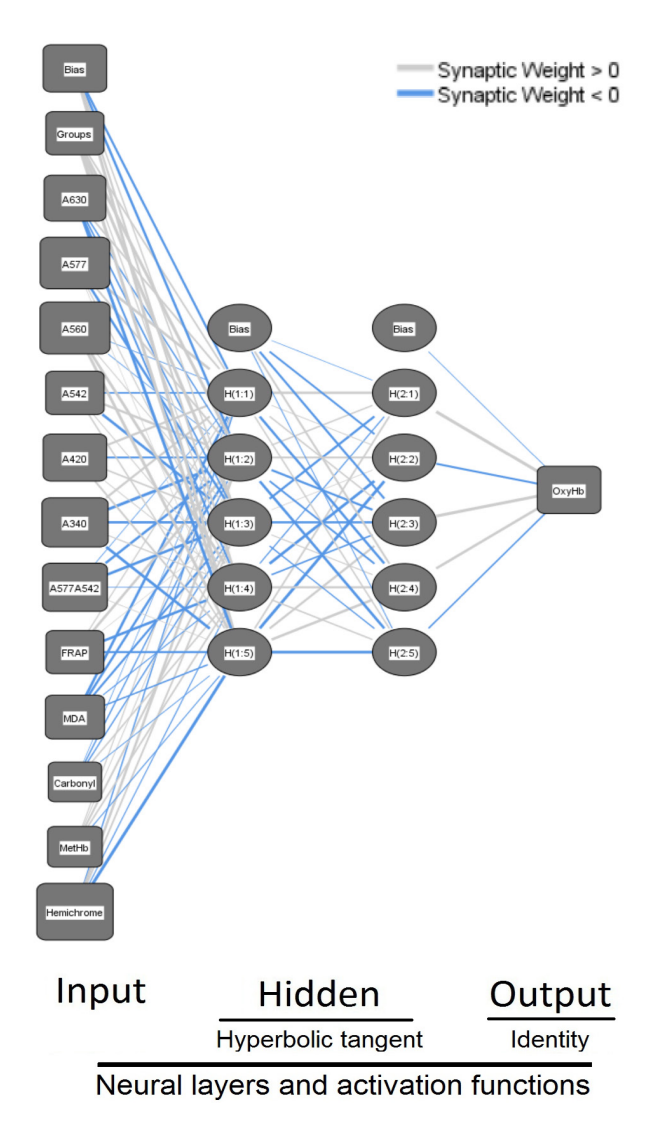


Figure 2. Feed-Forward Architecture of the Designed Artificial Neural Network. This Description diagram displays information about the designed artificial neural network, including the independent variables in input layer, Hb derivatives and biochemical parameters as dependent

5) HMC produces a shallower trough at 560 nm, 6) the heme-heme interaction band, known as the Soret band, is located at 420 nm, 7) the globin-heme interaction band is found at 340 nm, and 8) a constant globin band at 275 nm represents the dynamic motion of hemoglobin [25].

Antioxidant power of plasma

The FRAP assay, developed by Benzie and Strain (26), is used to measure the total antioxidant capacity of plasma. Briefly, the antioxidant agents reduce tripyridyltriazine complex (TPTZ- Fe3+) to ferrous (Fe2+) form which is blue in the acidic medium, with maximum optical absorption at 593 nm.

MDA content of plasma

MDA levels were measured using the TBARS method described by Buege and Aust (36). Plasma samples (20 µl) were mixed with TBA solution and were heated in boiling water for 45 minutes, then cooled and centrifuged at 550 g for 25 minutes. The absorbance of the supernatant pink solution was measured at 532 nm, and values were expressed as nmol/ml of plasma.

Protein carbonyl groups

The carbonyl assay was conducted by the method introduced by Evans (27). According to the method, 2,4-dinitrophenylhydrazine (DNPH) reacts with carbonyl groups to form 2,4-dinitrophenylhydrazone derivatives with maximum optical absorption at 380 nm.

Protein concentration was calculated as mg/ml according to compare with standard curve and related absorbance at 280 nm. The carbonyl content of plasma proteins was reported as nmol/ mg of protein concentration.

Statistical Analysis

Statistical analysis was performed using SPSS version 20, while Microsoft Excel 2010 was used for data classification. The mean and standard error of the mean (SEM) were calculated for each group. ANOVA was employed to compare the means of different groups, with a significance at the level of P < 0.05.

ANN analysis

ANN analysis was conducted to identify predictive

parameters by a four-layer perceptron method (13-5-5-1) according to automatic architecture selection. Hyperbolic tangent and identity functions were utilized as activation functions in the hidden and output layers, respectively. The selection of an appropriate results was based on R^2 , the sum of squared errors, and relative errors during training and testing phases. It is generally accepted that a suitable model should have an error rate below 0.02.

At each step of analysis a separate parameter was considered as predictive variable in output layer on other parameters were selected as independent variable. Hyperbolic tangent and identity functions were applied in hidden and output layers, respectively. During ANN analysis, 70% and 30% of data were randomly used in training and testing steps, respectively. To improve the training process of ANN analysis, the standardization method was used for rescaling the data by the following formula:

$Standardization\ indicator = (x\ mean)/SD$

It is worth noting that the residual by predicted chart should show no visible patters which indicates that the residuals are randomly distributed and the designed ANN model effectively captures the underlying data patterns without systematic errors. Also, there will be no evident bias in the predictions and that the variance of the residuals remains constant across all levels of the predicted values of the estimated parameters.

Ethical Statement

This study was conducted following approval from the Vice Chancellor for Research and Technology (Grant No. 2108) and the Ethics Committee of Arak University of Medical Sciences (Ethics Code 93-176-4). All stages of the study adhered to the guidelines of the Declaration of Helsinki. Also, all required laboratory health and safety protocols were followed throughout the research.

Results

Structural changes in Hemoglobin OxvHb

As Figure 3 shows, in the group with X-ray exposure, a significant reduction in oxyHb was observed from 35.37 ± 1.37 to 17.05 ± 1.25 µmol, which indicates a 41.46%

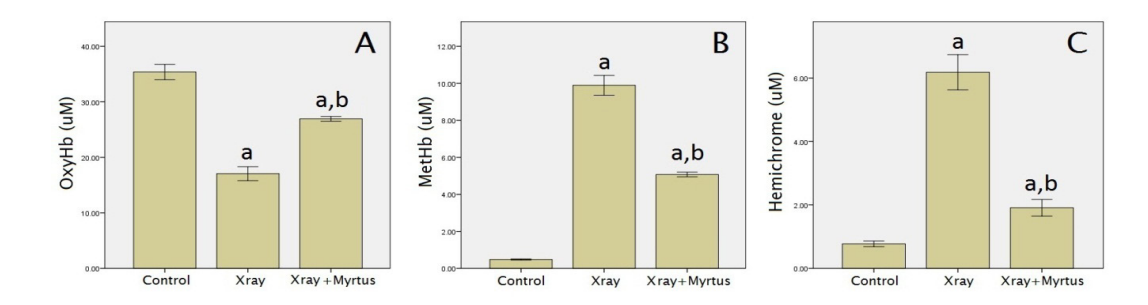


Figure 3. The Mean Values of oxyHb and Oxidative Derivatives of Hb. Results are presented as μ mol/L. Control groups: without any treatment, x-ray group: after exposure to x-ray radiation, x-ray+ Myrtus: after administration of Myrtus communis extract and exposure to x-ray. Error bars show SD and abbreviations a and b indicate significant difference between control and x-ray groups, respectively (P<0.05).

decrease in the erythrocyte capacity to carry oxygen (P< 0.001). Similarly, reduction of Hb optical absorption at wavelengths of 542 nm (Figure 4C) and 577 nm (Figure 4B) support a decline in the concentration of oxyHb.

The administration of the aqueous extract of Myrtus communis L. leaves to the rats which were exposed to X-ray resulted in a significant decrease in the concentration of oxyHb that indicates a 36.8% enhancement in the erythrocytes' ability to carry oxygen (Figure 3A). These findings suggest that Myrtus communis extract induces protective effects against oxidative effects of X-ray radiation. This conclusion is further supported by the notable rise of OxyHb concentration which is indicated by increase in Hb absorbances at 577 nm (Figure 4B) and 542 nm (Figure 4C) in the group that received the aqueous extract of Myrtus communis L. leaves (Figure 3).

Pearson correlation coefficients showed the significant positive effects of A577 (r=0.976), A542 (r+0.938), and A340 (r+0.910) and a significant negative effect of MDA (r=-0.951) on the concentration of OxyHb (Table 1).

The acceptable Squared Errors (SSE) and Relative Error (RE) of the designed ANN model for OxyHb were 0.027 and 0.003 in the training step and 0.082 and 0.031 in the testing step, respectively (Table 2). Also, the accuracy of our ANN model can be shown by the significant positive linearity (y=0.69+0.98x) and high R^2 value (0.991) of the predicted by observed chart for OxyHb concentration (Figure 6A). The ANN model indicated that HMC concentration and Hb absorbances at 560 and 577 nm were the three most important parameters for predicting the concentration of OxyHb (Table 3). The residual by predicted charts for the concentrations of OxyHb (Figure 6B) shows no visible patter.

MetHh

The results of this study indicate that changes in oxyHb concentration are associated with variations in the concentration of metHb and HMC. In the control group, the metHb level was measured at 0.48±0.03 µmol, which increased to 9.89±0.54 μmol after X-ray exposure, representing an 11.5-fold rise in hemoglobin oxidation

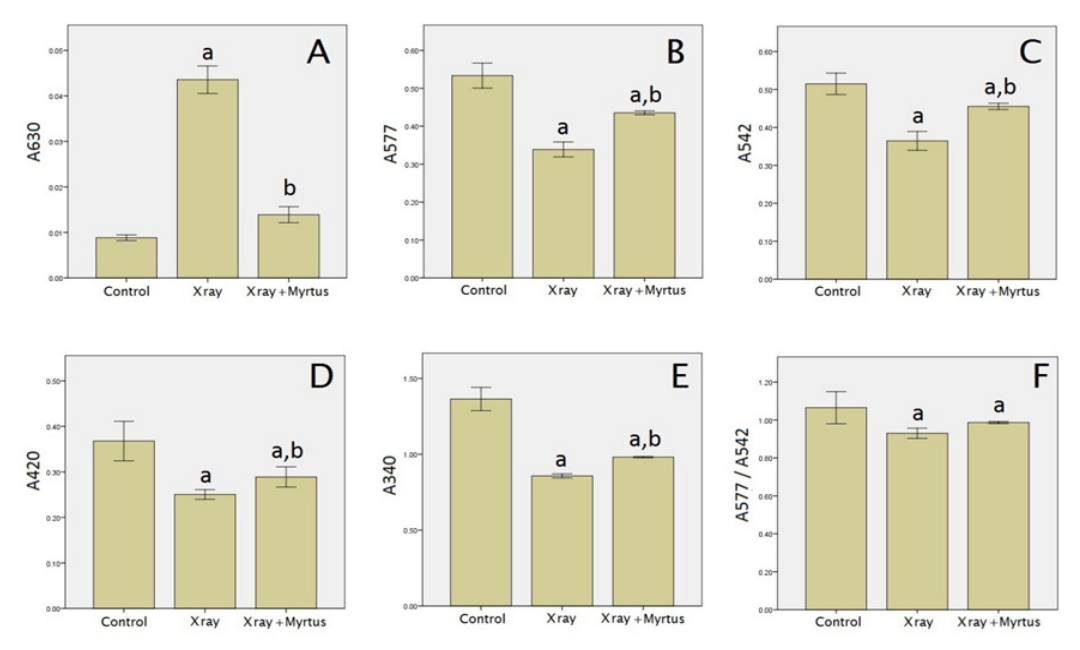


Figure 4. Comparison of Hb Absorbances at Different Wavelenghts. Control groups: without any treatment, x-ray group: after exposure to x-ray radiation, x-ray+Myrtus: after administration of Myrtus communis extract and exposure to x-ray. Error bars show SD and abbreviations a and b indicate significant difference from control and X-ray groups, respectively (P<0.05).

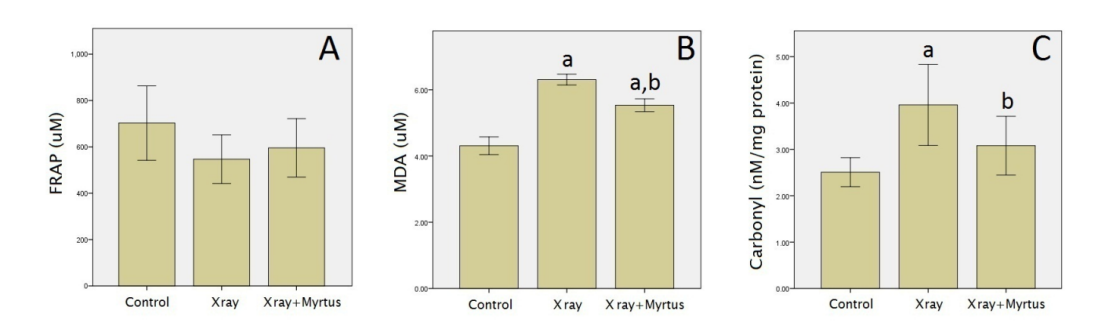


Figure 5. Antioxidant Power of Plasma and Oxidative Status of Proteins and Lipids in Plasma. The mean values of FRAP (A), MDA (B) and carbonyl (C) were compared between different groups. Control groups: without any treatment, x-ray group: after exposure to x-ray radiation, x-ray+ Myrtus: after administration of Myrtus communis extract and exposure to x-ray. Error bars show SD and a and b indicate significant differences (P<0.05) from control and x-ray groups, respectively. Abbreviations: FRAP: ferric reducing ability of plasma, MDA: malonyl dialdehyde, Carbonyl: carbonyl content of plasma proteins.

Table 1. Heat map of Pearson Correlation Coefficients. The Pearson correlation coefficients between Hb absorbances and plasma oxidant and antioxidant parameters are presented with emphasis on the negative (blue) and positive (red) correlations. The significances at the level \leq 0.001 are indicated by bold numbers.

	A630	A577	A560	A542	A420	A340	A577/A542	FRAP	MDA	Carbonyl	OxyHb	MetHb	HMC
A630	1												
A577	-0.861	1											
A560	-0.735	0.936	1										
A542	-0.88	0.933	0.827	1									
A420	-0.708	0.812	0.727	0.749	1								
A340	-0.737	0.891	0.799	0.825	0.91	1							
A577/A542	-0.656	0.802	0.806	0.565	0.619	0.739	1						
FRAP	-0.414	0.438	0.399	0.326	0.649	0.542	0.481	1					
MDA	0.812	-0.943	-0.853	-0.881	-0.876	-0.952	-0.758	-0.448	- 1				
Carbonyl	0.675	-0.741	-0.689	-0.722	-0.517	-0.618	-0.577	-0.214	0.731	1			
OxyHb	-0.888	0.976	0.886	0.938	0.848	0.91	0.762	0.434	-0.951	-0.707	1		
MetHb	0.886	-0.967	-0.866	-0.943	-0.852	-0.934	-0.748	-0.426	0.966	0.725	-0.992	1	i I
HMC	0.946	-0.896	-0.77	-0.91	-0.76	-0.798	-0.677	-0.4	0.864	0.657	-0.948	0.942	1

(Figure 3B). Conversely, treatment with the extract reduced the metHb level to 5.07±0.13 µmol, marking a 56% decrease and demonstrating the significant protective effect of Myrtus communis against hemoglobin oxidation.

A decrease in the A577/A542 ratio (Figure 4F) signifies the conversion of oxyHb to metHb. In the group exposed to X-ray, this ratio fell from 1.063 ± 0.084 to 0.93 ± 0.027 , indicating a 25% increase in the conversion of oxyHb to

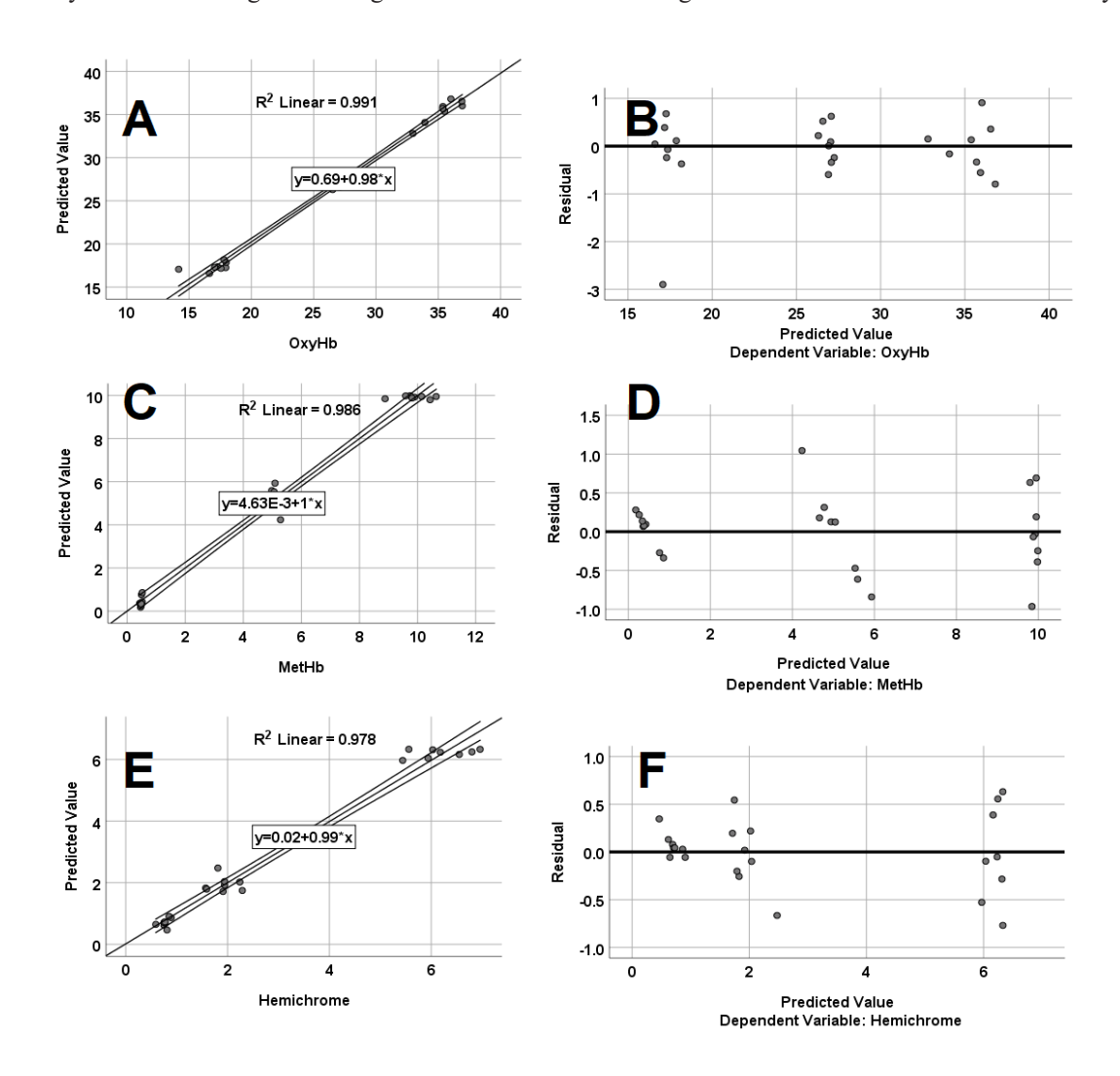


Figure 6. Predicted by observed (A) and residual by predicted (B) charts for Hb derivatives. There is a positive correlation between predicted and observed values (A) but no visible pattern between residuals and predicted values for each scale-dependent variable (B) in the artificial neural network. OxyHb: oxyhemoglobin.

Table 2. Model Summary of the Proposed ANN Model. The table displays a summary of the neural network performance including sum-of-squares errors (SSE), relative errors (RE) in training and testing steps and R2 of the predicted by observed equations. Error computations were based on the testing sample. Carbonyl: carbonyl content of plasma proteins, FRAP: ferric reducing ability of plasma, hemichrome: HMC, MDA: malonyl dialdehyde.

		OxyHb	MetHb	HMC	FRAP	MDA	Carbonyl
	SSE	0.027	0.088	0.157	0.385	0.919	1.853
Training	RE	0.003	0.011	0.021	0.051	0.097	0.285
	SSE	0.082	0.061	0.068	8.177	0.012	1.17
Testing	RE	0.031	0.023	0.039	0.802	0.004	0.493
Predicted by observed equation	\mathbb{R}^2	0.991	0.986	0.978	0.547	0.935	0.667

metHb. These findings align with the significant rise in optical absorption at 630 nm (Figure 4A), which indicates metHb formation. Administration of Myrtus communis extract to X-ray-exposed rats raised the A577/A542 ratio to 0.989±0.006, suggesting its protective effects against the conversion of oxyHb to metHb. Concurrently, hemoglobin optical absorption at 630 nm decreased, indicating a reduction in metHb concentration in erythrocytes, thereby confirming the protective effects of Myrtus communis extract. Pearson correlation coefficients showed the significant positive effects of MDA (r=0.966) and the significant negative effects of A577 (r=-0.967),

A542 (r=-0.943), A340 (r=-0.934), and OxyHb (r=-0.992) on the concentration of metHb (Table 1). The acceptable SSE and RE of the ANN model for metHb concentrations were 0.088 and 0.011 in the training step, and 0.061 and 0.023 in the testing step, respectively (Table 2). The model's accuracy is evidenced by the significant positive linearity and a high coefficient of determination between predicted and observed metHb concentrations (Figure 7C). The ANN model for predicting the metHb concentrations introduced A340, A577/A542, and A630 as the three most important parameters (Table 3). The residual by predicted charts for the concentrations of metHb (Figure 6D) shows

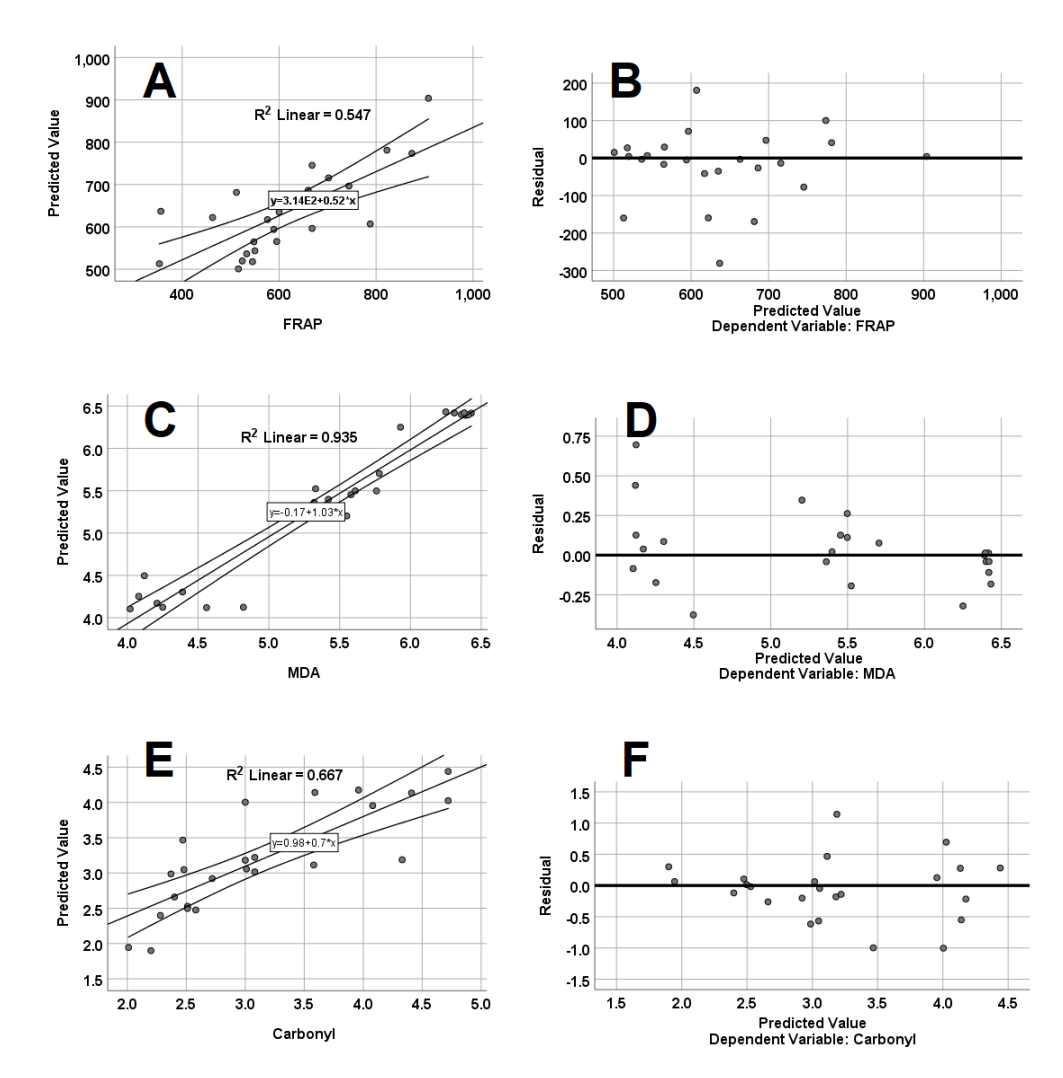


Figure 7. Predicted by observed (A) and residual by predicted (B) charts for plasma oxidative stress markers. There is a positive correlation between predicted and observed values (A) but no visible pattern between residuals and predicted values for each scale-dependent variable (B) in the artificial neural network. OxyHb: oxyhemoglobin.

Table 3. Independent Variable Importance Analysis. The chart performs a sensitivity analysis, which computes the percent of normalized importance of each independent parameter to estimate the concentration of Hb derivatives and plasma oxidative stress parameters. A: Hb absorbance at indicated wavelengths, Carbonyl: carbonyl content of plasma proteins, FRAP: ferric reducing ability of plasma, hemichrome: HMC, MDA: malonyl dialdehyde, MetHb: methemoglobin.

OxyHb		M	MetHb	Н	HMC	F	FRAP	7	MDA	Caı	Carbonyl
Independent Parameter	Normalized Importance (%)										
HMC	100.0	A340	100.0	OxyHb	100.0	A420	100.0	A577A542	100.0	A577	100.0
A560	74.8	A577A542	85.5	MetHb	96.8	A577A542	92.7	A340	77.4	A560	80.0
A577	73.1	A630	75.2	A542	59.5	MetHb	78.1	A577	50.8	MDA	71.6
A340	59.7	A560	49.7	A630	51.3	A542	56.6	A542	39.8	A577A542	55.2
A577/A542	54.7	A577	49.0	FRAP	34.2	MDA	50.4	OxyHb	36.6	HMC	46.5
A420	49.9	A542	39.8	A340	31.0	Carbonyl	38.5	A560	35.0	FRAP	40.9
A630	42.8	HMC	37.9	A577	27.8	HMC	37.0	A630	33.8	MetHb	34.5
MDA	32.1	MDA	32.1	A560	26.2	A560	28.2	Carbonyl	33.6	A420	33.4
A542	29.0	FRAP	23.7	A577A542	26.1	Groups	20.1	FRAP	30.7	A542	32.7
Groups	28.4	Groups	23.3	A420	23.1	A630	18.3	HMC	26.9	A340	21.7
FRAP	27.4	Carbonyl	20.8	Carbonyl	22.9	A577	17.7	MetHb	23.9	OxyHb	21.0
MetHb	14.8	A420	10.6	MDA	14.2	OxyHb	17.3	A420	14.7	Groups	21.0
Carbonyl	9.7	OxyHb	10.5	Groups	14.1	A340	14.6	Groups	10.9	A630	19.6

no visible patter.

HMC

In the control group, HMC concentration was 0.77 \pm 0.09 μ M, which rose to 6.18 \pm 0.55 μ mol following X-ray exposure, indicating a 14.7-fold increase in hemoglobin oxidation (Figure 3C). However, after administering the Myrtus communis extract, the HMC concentration decreased to 1.91 \pm 0.26 μ M, reflecting an 11.5-fold reduction in hemoglobin oxidation.

Our results indicated an increase in the optical density of hemoglobin at 630 nm, rising from 0.01±0.000 to 0.045 ± 0.005 (P < 0.05, Figure 4A). This change suggests the conversion of oxyHb to metHb in the X-ray group. This conversion demonstrates the oxidative effects of X-ray radiation on hemoglobin structure, leading to an increased concentration of metHb (P < 0.001), which in turn raises the HMC concentration (P < 0.001). Pearson correlation coefficients showed the significant positive effects of A630 (r=0.946) and metHb (r=0.942) and the significant negative effects of A542 (r=-0.910), and OxyHb (r=-0.948) on the concentration of HMC (Table 1). The SSE and RE of the ANN model for HMC concentrations were 0.157 and 0.021 in the training step, and 0.068 and 0.039 in the testing step, respectively (Table 2). The model's accuracy is evidenced by the significant positive linearity and a high coefficient of determination between predicted and observed HMC concentrations (Figure 6E). The ANN model for predicting the metHb concentrations indicated that the concentrations of oxyHb and metHb were the two most important parameters (Table 3). The residual by predicted charts for the concentrations of HMC (Fig ure 6F) shows no visible patter.

Hemoglobin Absorbances

The Soret band at 420 nm indicates heme-heme interactions within the hemoglobin structure. In the X-ray exposed experimental group, a significant decrease in the Soret band was noted, dropping from 0.37 ± 0.043 to 0.251 ± 0.01 (P < 0.05; Figure 4D). Following the administration of the Myrtus communis extract, optical absorption of Soret band increased to 0.290 ± 0.022 , indicating enhanced heme ring interactions and protective effects of Myrtus communis extract against oxidative damage from X-ray exposure (P < 0.05).

X-ray exposure also reduced hemoglobin optical absorption at 340 nm from 1.394 ± 0.077 to 0.858 ± 0.013 , signifying a 29.4% decline in heme-globin interactions (P < 0.05; Figure 4E). Notably, our results demonstrated a significant increase in hemoglobin optical absorption to 0.981 ± 0.006 after administering Myrtus communis extract in rats exposed to X-ray (P < 0.05). The reduction in absorbance at 340 nm suggests a weakening of the non-covalent bond between heme iron and the histidine residue. Additionally, significant decreases in absorbance values at 577 nm (Figure 3B) and 542 nm (Figure 4C), correlate with oxyHb concentration.

Antioxidant power of plasma

In the group exposed to X-ray, the FRAP level decreased from $703{\pm}161$ to $547{\pm}105~\mu\text{M}$, representing a

non-significant reduction of 14.3% in plasma antioxidant capacity compared to the control group (p = 0.07, Figure 5A). Also, administration of Myrtus communis extract prior to X-ray exposure induced a nonsignificant increase of 4.8% in the FRAP level which was still lower than the control group (p = 0.26, Figure 5A). Pearson correlation coefficients showed no significant effects of the estimated parameters on the FRAP values (Table 1). The SSE and RE of our designed ANN model for FRAP were 0.385 and 0.051 in the training step, and 8.177 and 0.802 in the testing step, respectively (Table 2). The model's accuracy is evidenced by the significant positive linearity and a high coefficient of determination between predicted and observed metHb concentrations (Figure 7A). The ANN model showed that A420, A577/A542, and metHb concentration were the two three most important parameters for predicting the FRAP values (Table 3). The residual by predicted charts for the FRAP (Figure 7B) shows no visible patter.

MDA content of plasma

As shown in Figure 54B, the MDA level in the control group was 4.31±0.27 μM and following X-ray exposure, increased to $6.31\pm0.16~\mu M$ (P < 0.05) which indicated that X-ray radiation causes oxidation of plasma lipids. Interestingly, the administration of Myrtus communis extract during X-ray exposure resulted in a significant decrease in MDA levels to 5.53±0.2 µM that reflecting a 12.33% reduction in the oxidative effects of X-ray on plasma lipids (p < 0.05). Pearson correlation coefficients showed the significant negative effects of A577 (r=-0.943), and A340 (r=-0.952) on the MDA content of plasma (Table 1). Our designed ANN model showed acceptable values of SSE (0.919 and 0.012) and RE (0.097 and 0.004) for predicting MDA content of plasma, respectively (Table 2). The model's accuracy is evidenced by the significant positive linearity and a high coefficient of determination between predicted and observed metHb concentrations (Figure 7D). The ANN model for predicting MDA indicated that A577/A542 and A340 were the two most important parameters (Table 3). The residual by predicted charts for the concentrations of MDA (Figure 7D) shows no visible patter.

Protein carbonyl groups

As shown in Figure 5C, the level of protein carbonyls (PCO) in the control group was 2.51 ± 0.31 nmol/mg of protein. Following X-ray exposure, this level increased to 3.96 ± 0.87 nmol/mg (P < 0.05), indicating that X-ray radiation causes oxidation of plasma proteins. However, the administration of Myrtus communis extract during X-ray exposure led to a significant reduction in carbonyl levels to 3.08 ± 0.63 nmol/mg, reflecting a 12.33% decrease in the oxidative impact of X-ray on plasma proteins (p < 0.05, Figure 4C).

Pearson correlation coefficients showed no significant effects of the measured parameters on the carbonyl content of plasma proteins (Table 1). The SSE and RE of the ANN model for carbonyl groups were 1.853 and 1.170 in the training step, and 0.285 and 0.493 in the testing step, respectively (Table 2). The model's accuracy is evidenced

by the significant positive linearity and a high coefficient of determination between predicted and observed metHb concentrations (Figure 7F). The ANN model for predicting the carbonyl indicated that A477, A560, and MDA content of plasma were the three most important parameters (Table 3). The residual by predicted charts for the carbonyl groups (Figure 7F) show no visible patters.

Discussion

The imbalance between increased reactive oxygen species (ROS) production and the body's antioxidant defenses leads to oxidative stress, which induces conformational changes in proteins and lipids. The extent of oxidative damage depends on the ROS source and concentration, as well as the efficiency of endogenous antioxidant mechanisms. In this study, whole-body exposure to X ray radiation significantly elevated protein carbonyl levels in rat plasma (Figure 3). Similar observations have been reported in previous studies: for instance, Srinivasan et al. demonstrated that ionizing radiation increases protein carbonylation in rat brain tissue via elevated ROS and reduced antioxidant enzyme activity [24]. Likewise, Han et al. [25] observed increased plasma protein carbonyls following gamma irradiation in mice.

We observed a significant increase in plasma malondialdehyde (MDA) following X ray exposure; plasma MDA positively correlated with metHb and heme—metHb complexes (HMC) levels and inversly with oxyhemoglobin (OxyHb) (Table 1, Figure 3). This finding aligns with Bouaziz et al., who reported that Myrtus communis extract reduced MDA levels and improved lipid profiles in hyperlipidemic rats [26]. Similarly, Sen et al showed that Myrtus communis extract boosts antioxidant defenses and lowers lipid peroxidation in bile-duct ligated rats [27]. These parallel findings support the efficacy of Myrtus communis in attenuating radiation-induced lipid oxidation.

Hemoglobin was also notably affected by irradiation, with increased metHb and HMC formation, and reduced OxyHb levels. These results support findings by Venkatesan et al., who documented radiation-induced hemoglobin oxidation and metHb accumulation [28]. Under oxidative stress, the balance between metHb production and reduction is disrupted, leading to metHb accumulation, heme degradation, and the formation of toxic species such as HMC, which can further promote oxidative stress and erythrocyte damage.

Treatment with Myrtus communis aqueous extract significantly reduced metHb and HMC levels, while restoring OxyHb and preserving heme spectral characteristics. These findings corroborate those of Sepici-Dinçel et al., who reported that Myrtus communis preserves erythrocyte integrity and resists oxidative hemolysis in diabetic rats [29]. Protective effects of the extract on hemoglobin structure, including normalization of Soret band (420 nm) and globin—heme interactions (577 nm), suggest stabilization of heme configuration and enhanced oxygen affinity, comparable to findings in Zhao et al, which showed plant-derived antioxidants can preserve hemoglobin function during oxidative stress [30].

The elevated protein carbonyls and lipid peroxidation concurrently observed are biologically plausible given the pseudo-peroxidase activity of metHb (oxidized Hb), which can generate ROS and propagate oxidative damage to proteins and membranes. These findings reinforce the concept that hemoglobin oxidation contributes to broader oxidative stress, as reported by Evans and Levine on protein oxidation in irradiated tissues [31].

Our results have important implications in X-ray radiotherapy for cancer patients, in whom the excessive amount of ROS and oxidative stress are characteristic features. The importance of erythrocyte as an experimental model cell for estimating of the oxidative damages has become evident from the conformational changes in Hb, including polypeptide subunits and heme moiety. In this work, an accurate and reliable algorithm of experiments was presented for estimating the ameliorative effects of Myrtus communis extract against X-ray induced oxidative stress. For this purpose, the response of erythrocytes to X-ray radiation and antioxidant properties of Myrtus communis extract against oxidative changes in Hb and plasma proteins and lipids have been investigated. Also, in the present study, an ANN analysis utilizing a multi-layer feed-forward learning algorithm was developed to identify the key parameters influencing oxyHb concentration. Our ANN model highlighted the significance of Hb absorbances at 577, 560, and 577 nm, as well as metHb and HMC concentrations, each contributing over 50% to the relative importance.

In conclusion, the findings of this study demonstrate that Myrtus communis aqueous extract exerts protective effects against X-ray-induced oxidative damage by preserving hemoglobin conformation and reducing lipid peroxidation and protein carbonylation in rat plasma. These protective effects are likely mediated through antioxidant mechanisms that stabilize the heme structure and maintain oxygen-binding functionality. Moreover, the application of artificial neural network (ANN) modeling enabled the identification of key spectrophotometric and biochemical parameters influencing hemoglobin oxidation, highlighting its potential utility in radiation biology research. Collectively, these results suggest that Myrtus communis extract may serve as a natural radioprotective agent, with potential therapeutic implications for reducing oxidative side effects in patients undergoing X-ray radiotherapy.

Author Contribution Statement

All authors contributed equally in this study.

Acknowledgements

This work was supported by the Research Council of Arak University of Medical Sciences under Grant Number 2108 and was conducted in accordance with ethics code 93-176-4.

Disclosure statement

The authors declare that they have no conflicts of

interest.

References

- 1. Thompson LH. Recognition, signaling, and repair of DNA double-strand breaks produced by ionizing radiation in mammalian cells: The molecular choreography. Mutat Res. 2012;751(2):158-246. https://doi.org/10.1016/j. mrrev.2012.06.002.
- 2. Ravanat J-L, Douki T. Uv and ionizing radiations induced DNA damage, differences and similarities. Radiation Phys Chem. 2016;128:92-102. https://doi.org/10.1016/j. radphyschem.2016.07.007.
- 3. Demir P, Akkas SB, Severcan M, Zorlu F, Severcan F. Ionizing radiation induces structural and functional damage on the molecules of rat brain homogenate membranes: A fourier transform infrared (ft-ir) spectroscopic study. Appl Spectrosc. 2015;69(1):154-64. https://doi.org/10.1366/13-07154.
- 4. Zhou Y, Ni H, Balint K, Sanzari JK, Dentchev T, Diffenderfer ES, et al. Ionizing radiation selectively reduces skin regulatory t cells and alters immune function. PLoS One. 2014;9(6):e100800. https://doi.org/10.1371/journal. pone.0100800.
- 5. Manna K, Das U, Das D, Kesh SB, Khan A, Chakraborty A, et al. Naringin inhibits gamma radiation-induced oxidative DNA damage and inflammation, by modulating p53 and nf-κb signaling pathways in murine splenocytes. Free Radic Res. 2015;49(4):422-39. https://doi.org/10.3109/10715762 .2015.1016018.
- 6. Mothersill C, Rusin A, Seymour C. Low doses and non-targeted effects in environmental radiation protection; where are we now and where should we go? Environ Res. 2017;159:484-90. https://doi.org/10.1016/j.envres.2017.08.029.
- 7. Guo J, Zhao D, Lei X, Zhao H, Yang Y, Zhang P, et al. Protective effects of hydrogen against low-dose long-term radiation-induced damage to the behavioral performances, hematopoietic system, genital system, and splenic lymphocytes in mice. Oxid Med Cell Longev. 2016;2016:1947819. https://doi.org/10.1155/2016/1947819.
- 8. Martling A, Smedby KE, Birgisson H, Olsson H, Granath F, Ekbom A, et al. Risk of second primary cancer in patients treated with radiotherapy for rectal cancer. Br J Surg. 2017;104(3):278-87. https://doi.org/10.1002/bjs.10327.
- 9. Shirazi A, Mihandoost E, Mohseni M, Ghazi-Khansari M, Rabie Mahdavi S. Radio-protective effects of melatonin against irradiation-induced oxidative damage in rat peripheral blood. Phys Med. 2013;29(1):65-74. https://doi. org/10.1016/j.ejmp.2011.11.007.
- 10. Arora R, Gupta D, Chawla R, Sagar R, Sharma A, Kumar R, et al. Radioprotection by plant products: Present status and future prospects. Phytother Res. 2005;19(1):1-22. https:// doi.org/10.1002/ptr.1605.
- 11. Seed TM. Radiation protectants: Current status and future prospects. Health Phys. 2005;89(5):531-45. https://doi. org/10.1097/01.hp.0000175153.19745.25.
- 12. Painuli S, Kumar N. Prospects in the development of natural radioprotective therapeutics with anti-cancer properties from the plants of uttarakhand region of india. J Ayurveda Integr Med. 2016;7(1):62-8. https://doi.org/10.1016/j. jaim.2015.09.001.
- 13. Forman HJ, Davies KJ, Ursini F. How do nutritional antioxidants really work: Nucleophilic tone and parahormesis versus free radical scavenging in vivo. Free Radic Biol Med. 2014;66:24-35. https://doi.org/10.1016/j. freeradbiomed.2013.05.045.
- 14. Shahidi F, Ambigaipalan P. Phenolics and polyphenolics

- in foods, beverages and spices: Antioxidant activity and health effects - a review. J Funct Foods. 2015;18. https:// doi.org/10.1016/j.jff.2015.06.018.
- 15. Baliga MS, Jagetia GC, Venkatesh P, Reddy R, Ulloor JN. Radioprotective effect of abana, a polyherbal drug following total body irradiation. Br J Radiol. 2004;77(924):1027-35. https://doi.org/10.1259/bjr/83720350.
- 16. Jothy SL, Saito T, Kanwar JR, Chen Y, Aziz A, Yin-Hui L, et al. Radioprotective activity of polyalthia longifolia standardized extract against x-ray radiation injury in mice. Phys Med. 2016;32(1):150-61. https://doi.org/10.1016/j. ejmp.2015.10.090.
- 17. Hayder N, Abdelwahed A, Kilani S, Ammar RB, Mahmoud A, Ghedira K, et al. Anti-genotoxic and free-radical scavenging activities of extracts from (tunisian) myrtus communis. Mutat Res. 2004;564(1):89-95. https://doi. org/10.1016/j.mrgentox.2004.08.001.
- 18. Rosa A, Deiana M, Casu V, Corona G, Appendino G, Bianchi F, et al. Antioxidant activity of oligomeric acylphloroglucinols from myrtus communis l. Free Radic Res. 2003;37(9):1013-9. https://doi.org/10.1080/1071576 0310001595739.
- 19. Aidi Wannes W, Mhamdi B, Sriti J, Ben Jemia M, Ouchikh O, Hamdaoui G, et al. Antioxidant activities of the essential oils and methanol extracts from myrtle (myrtus communis var. Italica l.) leaf, stem and flower. Food Chem Toxicol. 2010;48(5):1362-70. https://doi.org/10.1016/j. fct.2010.03.002.
- 20. Hayder N, Skandrani I, Kilani S, Bouhlel I, Abdelwahed A, Ben Ammar R, et al. Antimutagenic activity of myrtus communis 1. Using the salmonella microsome assay. S Afr J Bot. 2008;74:121. https://doi.org/10.1016/j. sajb.2007.10.001.
- 21. Jabri MA, Rtibi K, Ben-Said A, Aouadhi C, Hosni K, Sakly M, et al. Antidiarrhoeal, antimicrobial and antioxidant effects of myrtle berries (myrtus communis l.) seeds extract. J Pharm Pharmacol. 2016;68(2):264-74. https://doi.org/10.1111/ jphp.12505.
- 22. Ines S, Ines B, Wissem B, Mohamed BS, Nawel H, Dijoux-Franca MG, et al. In vitro antioxidant and antigenotoxic potentials of 3,5-o-di-galloylquinic acid extracted from myrtus communis leaves and modulation of cell gene expression by h2o2. J Appl Toxicol. 2012;32(5):333-41. https://doi.org/10.1002/jat.1655.
- 23. Tumen I, Senol FS, Orhan IE. Inhibitory potential of the leaves and berries of myrtus communis l. (myrtle) against enzymes linked to neurodegenerative diseases and their antioxidant actions. Int J Food Sci Nutr. 2012;63(4):387-92. https://doi.org/10.3109/09637486.2011.629178.
- 24. Srinivasan A, et al. Ionizing radiation induces protein carbonylation via ros-mediated mechanisms. Free Radic Res.44:1-9.
- 25. Han J, et al. Plasma protein oxidation following gamma irradiation in mice. Radiat Res. 180:123-31.
- 26. Bouaziz m, et al. Myrtus communis extract reduces lipid peroxidation in hyperlipidemic rats. Ethnopharmacology.132:581-90.
- 27. Sen a, et al. Antifibrotic and antioxidant effects of myrtus communis in liver injury. J Ethnopharmacol. 189:200-8.
- 28. Venkatesan p, et al. Gamma radiation-induced hemoglobin oxidation and methemoglobin formation. Radiat Biol. 89:311-8.
- 29. Sepici-dincel a, et al. Protective effects of myrtus communis on erythrocytes in diabetic rats. Phytomedicine. 14:787–92.
- 30. Zhao 1, et al. Plant-derived antioxidants preserve hemoglobin function under oxidative stress. Journal of radioprotection.73:232–40.

31. Evans p, levine rl. Radiation-induced protein oxidation in tissues. Arch Biochem Biophys. 488:260-7.



This work is licensed under a Creative Commons Attribution-Non Commercial 4.0 International License.